Chapter 6:

pH Reversible Graphene Oxide-protein Bioconjugates with Proteolysis-Resistance Properties for Biomedical and Drug Delivery Applications

6.1 Introduction

6.1.1 Interaction of Graphene Oxide with Biomolecules

Single-layer graphene is constituted by tightly packed carbon decorated in a uniform 2D honeycomb lattice of a large surface area. After its discovery in 2004 [1], it gained a wide interest in new-age technology applications because of a high surface area:volume ratio, and strong mechanical properties. Most applications focussed on the nanoelectrical properties of graphene like ultrafast transistors and ambipolar memory devices [2]. An inexpensive hydrogel was synthesized using graphene and amyloid which could be used as a humidity sensor, was enzyme degradable and conducting as well [3]. Oxidation of graphene, yields GO as a derivative, which possesses outstanding physicochemical properties like water solubility and more biocompatibility. This happens because sp^3 domains readily accommodate pendant groups like epoxy, hydroxyl on the basal plane and carboxylic acid on the edges which help in alleviating hydrophobicity, increasing solubility, amphiphilicity and in covalent functionalization for specific applications [4]. As-such it has attracted extensive research interest especially in tissue engineering and biomedicine for crafting sensors, imaging probes, diagnostics, antibacterial and novel functional materials, tumor therapy and drug delivery [5]. GO has been functionalized using alkyl chains, amino acids and linear polymers [6]. Still a comprehensive understanding of the interaction of such nanomaterials with biomolecules is needed in greater detail

for exploitation in potential utilities. It is an excellent support for various nanoparticles [7].

6.1.2 Attachment of Proteins and DNA to the GO Surface Through Non-covalent Bonds

Presence of functional groups and aromatic domains enables GO to be used as a substrate in biochemical sensing through the formation of noncovalent bonds like H-bonding, hydrophobic interactions, π–π stacking, and electrostatic interactions. GO has been found to mimick enzymes for instance by inhibiting α-chymotrypsin to affect reaction processes [8]. Nucleobases of single-stranded DNA stack over GO via hydrogen bonding and π–π stacking which is prohibited in double-stranded DNA [9]. Proteins are indispensible fundamental elements in physiological processes in which they play dominant roles. It is very essential to shed some light on protein-GO interactions for understanding the structural and functional changes caused by such binding. Molecular dynamics (MD) simulations are often used to develop a virtual understanding of these interactions at the atomic level. This ensures a better understanding of the dynamic molecular processes that otherwise are not easily captured through experimental techniques. MD simulations have shown that at certain spatial orientations, the sharp edges of graphene may pierce through protein dimers disrupting the non-covalent interactions and the cell membrane [10]. On the contrary it has been shown to protect the nucleotides from nucleases [10, 11]. The thickness of GO in comparison to pristine graphene, contributed by the higher oxidation level lends some steric effect to the nanosheet surface to be more biocompatible. Only at the initial contact time, may GO affect the cell membrane resulting in minute cytotoxicity [2, 12]. Some results for the affinity of amino acids with GO have shown the following sequences- [His> Trp> Tyr > Phe], [His > Tyr > Trp > Phe] and [Arg > His

> Lys > Trp > Tyr > Phe] depending on the parameters used during the process [7, 13, 14]. Peptides like hepcidin have been observed to show conformational changes when in the vicinity of graphene as compared to graphene oxide predicting the toxicity level [15]. Amino acids may lose their β-sheet structure because of intermolecular van der Waals and electrostatic interactions overpowering the intramolecular hydrogen bonds and other forces. Proteins may act as excellent adhesives between molecules [12, 16].

6.1.3 Techniques and Strategies Employed for Shedding Light on Protein-GO Interactions

Due to the "get-together effect", the neighboring atoms of the oxidised carbon become unstable and more prone to oxidation, thus creating patches of hydrophobic and hydrophilic regions on the GO surface [10, 17]. Attachment of amino acids on the surface of GO causes certain changes in the structural and electronic properties, this sensitivity can be harnessed for biosensing [7, 18]. Many techniques have been used to study GO-protein interactions in several reports. FRET and SPR techniques have often been employed to design GO-biomolecule systems for sensing applications [13,19,20]. The carboxylic group of GO can be covalently bound to the amino terminal of a protein by using activating agents as EDC/NHS [19,21]. Other reports, mainly focus on the non-covalent interactions between GO and proteins as it is a facile, reversible and spontaneous strategy. Electrostatic and π−π interactions have often been reported to be responsible for the GO affinity to amino acids. Highest stability has been observed for tryptophan and arginine with GO hinting at electrostatic and hydrophobic/ π−π interactions [14]. Lysozyme has been observed to strongly adsorb on GO. The interaction was found to be so strong that further separation became challenging [9,11,13]. In a report, BSA and lysozyme adsorbed on modified carbon nanotubes (CNTs) that resulted in the alteration of the secondary structures [9]. Van

der Waal's forces have also been seen to contribute to the insertion process of GO into a protein molecule. ITC (Isothermal Titration Calorimetry) experiments also affirmed interactions with positively charged polar amino acids but no significant interactions with non-polar and anionic amino acids suggesting the role of electrostatic and π–π interactions via oxygenated groups and aromatic domains of GO [14, 22]. Similar evidence from XPS has also been observed with amino acids. Histidine being weakly cationic has been observed to behave more like the aromatic amino acids and bind to GO through π–π interactions rather than electrostatic interactions [14]. These non-covalent interactions are important for the protein to form secondary and tertiary structures, interact with other proteins and receptor-ligand kind of roles.

Bigger the GO surface, lesser oxygenated it is, making it more amenable for forming hydrophobic bonds and π–π interactions with molecules like common drugs with complex rings. Heparin has been reported to strongly bind with GO via hydrophobic interactions [8, 23]. Smaller GO surfaces are bestowed with higher charge density and propensity for forming electrostatic bonds with molecules. Mostly fluorescence titration and concentration differential studies have been done to understand protein-GO interactions. GO has been observed to show better adsorption of proteins than rGO due to the hydrophilic polar functional groups making it an ideal adsorbent material in analytical chemistry [18]. Increasing the protein concentration increases the total protein content adsorbed by GO but the adsorption efficiency declines. Therefore lower concentrations of protein can be used for basic experiments requiring a good amount of proteins on the GO surface. Different proteins get adsorbed differently by GO [12, 18], this property can be used to magnetically separate or purify proteins based on selectivity. Although reports on the interaction of GO with proteins, peptides and amino acids are available, no systematic experimental

study has been done to show the validity of such an interaction. Using this information, the strong interaction of proteins with GO can be utilized for sustained drug (protein itself) release.

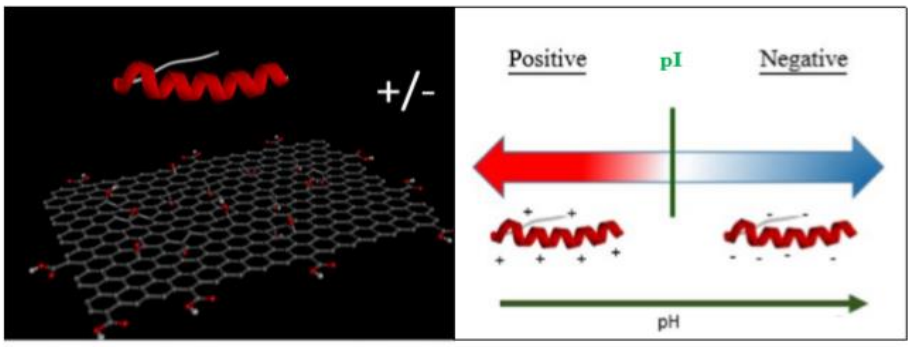

Figure 6.1: The Electrostatic Interactions between Proteins and GO

6.1.4 Biological Response and Applications of GO

GO possesses excellent bio-physico-chemical properties, like water solubility and biocompatibility *in vitro* and *in vivo* making it a versatile substrate for biological and biomedical applications such as biosensing, cellular imaging, controlled drug delivery, photothermal anticancer and antithrombotic therapy. Most of these applications depend on GO-protein bio-inorganic interface interactions. Proteins have a prominent physiological presence through a diverse range having different sizes, structures, compositions and concentrations. As such, when any nanomaterial like GO enters a physiological environment, it immediately comes in contact with proteins and this interaction depends on the surface properties of the material like hydrophilicity, surface charge and energy, biological response and dimensions. The association of GO with protein may modify the biological properties of GO by the better cellular uptake or cell signalling pathway activation processes offered by the adhered protein on the GO surface. Lack of a comprehensive understanding highly limits their biomedical applications. Therefore, a deeper understanding of these interaction mechanisms is

required before extending to the physiological state for practical use and to understand the influence of GO on the physiological changes of proteins. Interaction of GO with proteins is inevitable *in vivo* as soon as it comes in contact with the blood plasma with respect to nature, lateral size of GO and specificity. Majorly, proteins adsorb on GO through electrostatic interactions with different stability while van der Waal's also play a dominant role with rGO in addition to electrostatic interactions [8, 9, 22, 24]. For that reason, in this work, it is aimed to unfold the understanding on the role of electrostatic interactions in GO-protein affinity and formation of conjugates. *In vitro* studies using an array of biophysical techniques have been performed. Based on these studies, GO-protein pH-dependent conjugate phenomenon was determined.

6.2 Results and Discussions

In this chapter, efforts to elucidate the interactions of a common ubiquitously found biomolecule with graphene oxide sheets have been made. Systematically, graphene oxide has been checked for the formation of visible conjugates with amino acids, peptides and proteins. The role of charges on the surface of these molecules has been examined for the formation of these conjugates.

6.2.1 Graphene Oxide and its Interaction with Amino Acids

The procured highly uniform graphene oxide was assessed for the signature Raman markers commonly known as the D and G bands whose ratio gives an idea about the disorder in the carbon lattice (Figure 6.2A). It can be inferred from the graph, that the sheets are highly disordered with the incorporation of ether, hydroxyl and carboxyl groups on the surface and periphery of the sheets. At pH 2, pH 5 and pH 7 the DLS plot of graphene oxide alone in buffers was calibrated to see any change in the average sheet size (Figure 6.2B&C). No significant shift in peak was observed in

the DLS plot indicating no aggregation of sheets over the pH range. The correlation curve coincides well at every pH tested showing no change in size. Initially, five charged amino acids were incubated with graphene oxide (0.125mg/ml) at pH 3 (Figure 6.2B). Clearly, increase in size was evident by the DLS plot and correlation curves for only for the positively charged amino acids (arginine, lysine and histidine) but the peak stayed at the same coordinate as GO when negatively charged amino acids were added (aspartic acid and glutamic acid). Figure 6.2F clearly demonstrates the cause for the increase in size. No conjugates are seen in the upper row of amino acids- graphene oxide at pH 7, nor for the negatively charged amino acids at pH 3 shown in the lower row. However, clear visible aggregates can be seen when the positively charged amino acids and graphene oxide are incubated together at pH 3 which form spontaneously.

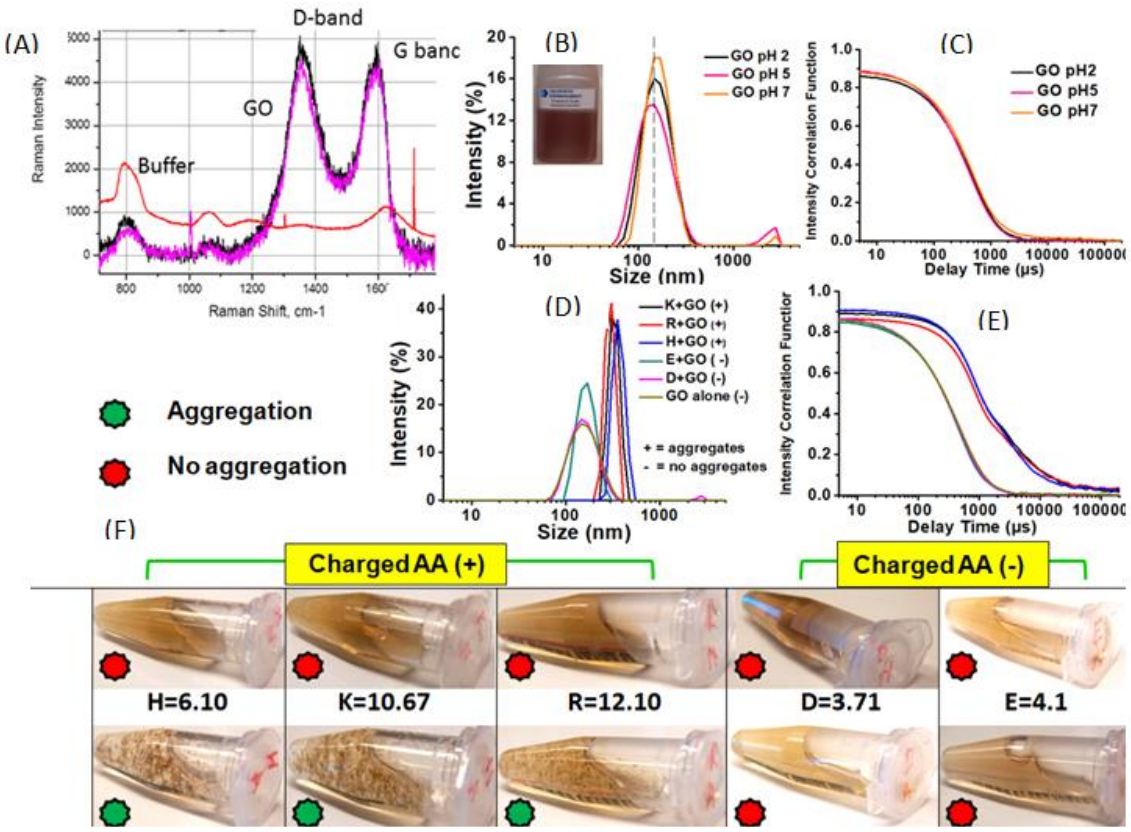

Figure 6.2: Interaction of Graphene Oxide with Charged Amino Acids. (A) Raman Spectroscopy of Graphene Oxide (B) DLS plot and (C) DLS correlation plot of Graphene oxide at different pH (D) DLS plot and (E) correlation plot of charged amino acids interacting with with graphene oxide at pH 3 (F) Formation of aggregates in only the positively charged AA-graphene oxide solution at pH 3

All the rest of the amino acids were subjected to the same pH conditions incubated with graphene oxide. No change in appearance was noticed for any other amino acid as seen in Figure 6.3A. This was supported by the light scattering data for size estimation which invariably remained the same (Figure 6.3B&C). These results suggest that there is a definitive involvement of weak ionic interactions resulting from the oppositely charged moeties, the positively charged amino acids and the negatively charged graphene oxide at a pH value which is below the pKa of the said amino acid. It is more protonated to yield a higher attractive force at lower pH, rapidly forming sandwiched layers of amino acid and GO sheets alternatively. Through the DLS

correlation curve, it was observed that when lysine was incubated at different pH, it readily formed conjugates with graphene oxide at acidic pH 2 and 5 but not so well at pH 7 as it was closer to its pKa value of 10.67 (Figure 6.3D). A remarkable phenomenon that was observed was the pH reversibility of the amino acid-graphene oxide conjugate formation. When histidine-GO buffer solution was subjected to a low pH of 3, the conjugates readily formed. As the pH was gradually increased, the conjugates visibly dissolved into a free solution. On reversing the pH, the conjugates reappeared making it a pH reversible phenomenon (Figure 6.3E). Histidine is a queer amino acid with pKa values of 1.78, 5.97 (imidazole) and 8.97. It becomes quite deprotonated above a pH value of 7 because of which the ionic attraction holding the conjugate weakens and it dissoves again into the solution.

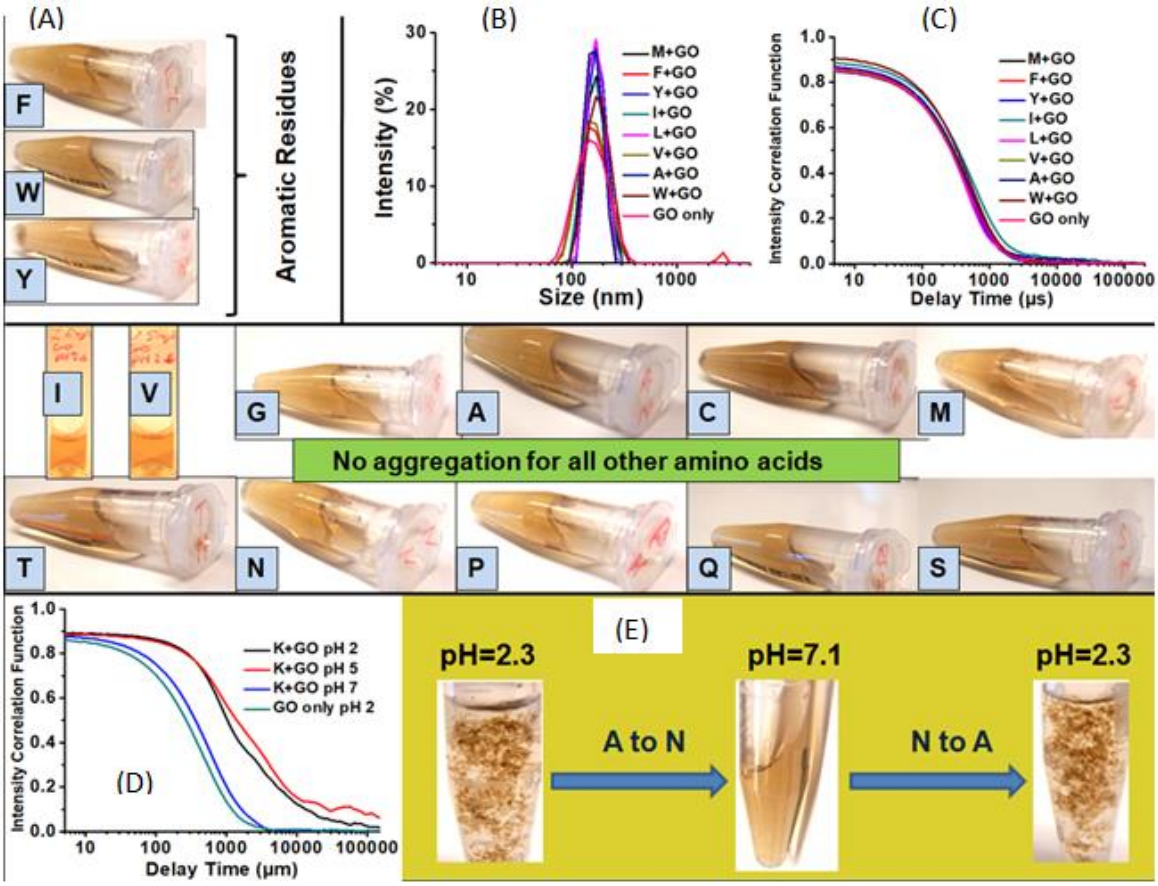

Figure 6.3: Interaction of Graphene Oxide with Amino Acids. (A) No aggregate seen for any other amino acid (B) DLS plot and (C) DLS correlation plot of other amino acids interacting with with graphene oxide at pH 3 (D) DLS correlation curve for lysine at different pH (E) the pH reversibility of histidine-graphene oxide solution for the formation of clearly visible conjugates

6.2.2 Assessment of GO-Peptide Interactions for Conjugate Formation

To gain a more structured perspective on the formation of AA-GO conjugates, peptide sequences bearing differential charges were designed. Peptides bearing net positive and net negative charges at different pH were designed along with hydrophobic and neutral peptides. The list of all peptides used is given in the table below.

Table 6.1: List of peptides used for observing peptide-GO conjugate formation through ionic interactions

S. NO.	Peptide Name	Peptide Sequence	Net Charge (pH2)
1	Peptide A	PKGPKGPKGKOGPDGDOGDOGDOGPKGPKG	++
2	Peptide B	PDGDOGDOGDOGPDGKOGPDGPDGPDGDOG	-
3	Peptide C	KOGPDGPDGPKGKOGPKGKOGKOGKOGKOG	+
4	Peptide $(PPG)_{10}$	PPGPPGPPGPPGPPGPPGPPGPPGPPGPPG	+
5	Peptide $(POG)_7AH$	POGPOGPOGPOGPOGPOGPOGAH	-
6	Peptide PH	POGPOGPOGPOGPOGPOGPOGPH	+

Three charged peptides (peptide A, peptide B and peptide C) were kept in two buffers incubated with GO at pH 2.3 and 7. At lower pH, all three peptides showed the formation of aggregates because of the net positive charge on the peptide by the protonated groups. However, at pH 7, peptide B did not form conjugates as opposed to peptide A and peptide C (Figure 6.4A). The most evident explanation lays in the fact that peptide B is richly constituted by negatively charged amino acids which give it an overall negative charge at pH 7 and no ionic attraction between both negatively charged peptide and GO. Peptide A and peptide C are still more protonated at pH 7 to form weak ionic interactions with GO capable of forming the visible conjugates. Other peptides did not readily form conjugates because of higher hydrophobicity and paucity of charges. To conclusively assess the role of ionic interactions, the zeta potential of all peptides was calibrated along with GO alone at different pH (Figure 6.4B). It was seen that Peptide A and Peptide C possessed a positive surface charge till neutral pH

unlike Peptide B, Peptide $(PPG)_{10}$ and Peptide $(POG)_7AH$. Graphene oxide showed a negative zeta potential over the whole pH range. This data definitively confirms the reason for the spontaneous conjugation of peptide-GO having a net positive surface charge by favouring strong ionic interactions.

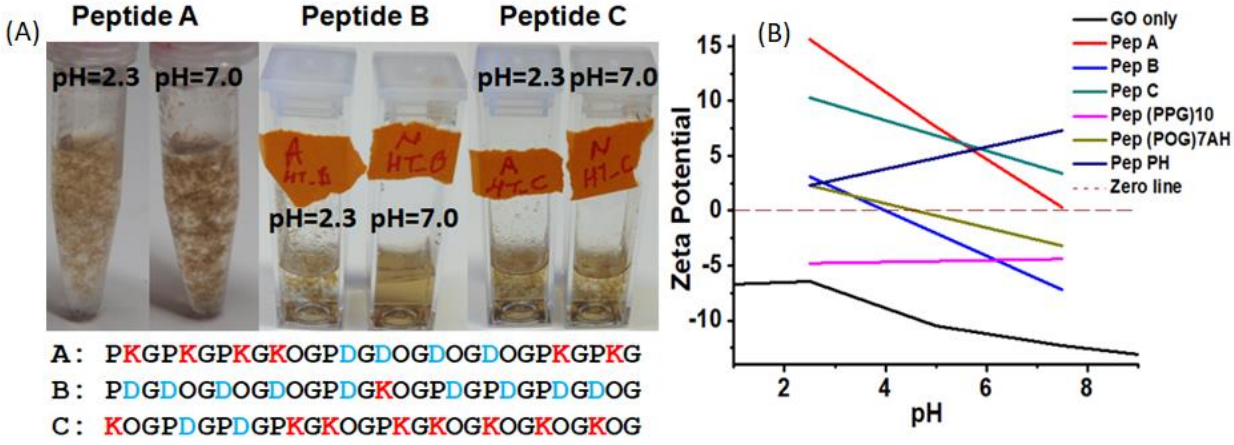

Figure 6.4: Interaction of GO with peptides for conjugate formation (A) Interaction of GO with Peptide A, Peptide B and Peptide C at pH 2.3 and pH 7 (B) Zeta potential of peptides and GO over a middle pH range

6.2.3 The Interaction of GO with Proteins to Check the Formation of Conjugates

To further extend the understanding of these conjugates in tertiary structures, model proteins were tested. Two model proteins, BSA (Bovine Serum Albumin) and lysozyme were incubated with GO at different pH. Surprisingly, no conjugates were observed for any pH value when protein and GO were incubated together. After heating the mixture just above the melting temperature of these proteins (70°C-BSA and 80°C-lysozyme) again similar spontaneous formation of aggregates was observed for both the proteins. This suggests that in the folded state, the functional groups on the surface of the constituent amino acids are occupied in forming weak bonds responsible for holding the tertiary organisation of the protein intact. The pI of the protein was an important consideration for the formation of GO-protein conjugates.

To check the protein content involved in the conjugate formation, the samples were centrifuged at 5000 rpm for 5 minutes to collect the conjugates in the pellet and measure the absorbance values of the supernatant to see the protein concentration. The conjugate structures did not hold against the shear stress due to the centrifugal force and broke into its former state causing anomalous absorbance readings (Figure 6.5A). This showed that these conjugate structures are temporary and weakly bound due to ionic interactions and can easily dissociate by applying a force. Lysozyme propelled more optically prominent GO-protein conjugates as compared to BSA. It did not form any conjugates in acidic or neutral pH (pH 3 and pH 7 respectively) but readily displayed them after unfolding at a high temperature of 95°C (Figure 6.5B). On the other hand, BSA shower smaller clusters in the conjugate positive samples which were markedly visible below its pI of 4.7 (Figure 6.5C). Interestingly, the zeta potential readings also correlated well with the hypothesis that at lower pH both proteins show a positive surface charge enabling better ionic coordination with the negatively charged GO sheet surface. On the other hand, as the pH increases, the zeta potential non-linearly regress towards an electronegative gradient (Figure 6.5D). While BSA shows a net negative zeta potential pH 5 onwards, lysozyme has a net positive surface charge even at pH 8. This explains why lysozyme more readily forms conjugates by having more positive zeta potential over most pH and its small size packs better between GO sheets.

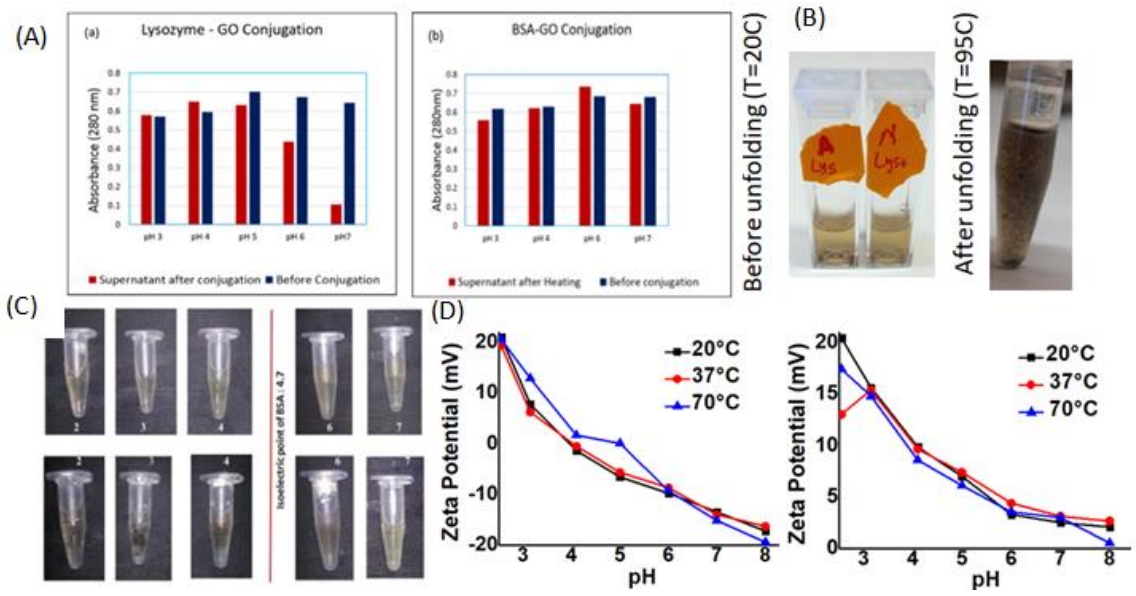

Figure 6.5: Investigation of GO-protein conjugates using BSA and lysozyme. (A) Supernantant absorbance values of lysozyme and BSA conjugates with GO at different pH before and after conjugation (B) Picture demonstrating that unfolding of the tertiary structure of protein is very important for the formation of protein-GO conjugates (C) Picture showing the role of pI of BSA (4.7) is very important for the formation of protein-GO conjugates as the functional groups are more protonated below the pI (D) Zeta potential of BSA and lysozyme respectively at different pH values

Different proteins were selected to test the efficacy of spontaneous formation of the GO-protein conjugates at three different temperatures. Globular proteins were selected for comparison which included insulin, chymptrypsin, trypsin, pepsin and tropomyosin. These proteins were subjected to different pH (2.55, 5.0, 7.0) and temperatures (20°C, 37°C, 70°C) to observe the zeta potential trend (Figure 6.6A-C). In general, all proteins show a peak decrement from a positive zeta potential to a negative zeta potential with the rise in pH values. As the incubation temperature of tropomyosin increases, the zeta potential range minimizes. On the other hand, for insulin, as the protein incubation temperature is increased, expansion in the zeta potential range for all three pH values is seen. Similar but very slight effect of incubation temperature is observed with pepsin. Trypsin and chymotrypsin do not

show a significant difference in the zeta potential values for different protein incubation temperatures. Strikingly, at 70°C, the protein structures unfolds to expose electronegative charges on the surface of both these proteins which might earlier have been involved in holding the tertiary structure. All modifications in zeta potential trend for all proteins indicate structural changes that may have been caused by the temperature and pH conditions. These changes may be temporary or permanent depending on the extent of protein unfolding and denaturation. This information can be gathered by the assessment of CD plots of proteins by tracing their ellipticity signals on reversing the temperature conditions and changing the pH of the solution. For this purpose, insulin was picked as it has a good balance of α helices and β sheets. The CD plot for insulin kept at pH 7 was recorded. Slowly the pH was dropped to acidic pH 2.8 and then raised to pH 7 again (Figure 6.6D). Both the spectra are almost coinciding with a minor deviation which indicates that the quarternary structure of insulin was intact after the pH phasing with slight bond shifts. Insulin at pH 2.8 (pI=5.33) was subjected to a heat cycle by initially keeping it at 4°C. Slowly its incubation temperature was increased to 70°C at which the globular structure changed into a molten state (Figure 6.6E). Again, the temperature was brought down to 4°C to restore its initial quarternary conformation. The restored structure has insignificant variation from the previous form and the α helices/ β sheets are seen to reappear. The spectra show a positive peak at 195 nm and negative peaks at 208 nm, 218 nm and 222 nm confirming the presence of secondary structures in the protein. From this data, it can be concluded that changes in pH and temperature required for the effective formation of GO-protein conjugates does not drastically alter the native structure of the protein and therefore these conjugates can be effectively used to exploit the symbiotic advantages of shielding GO and a functional protein.

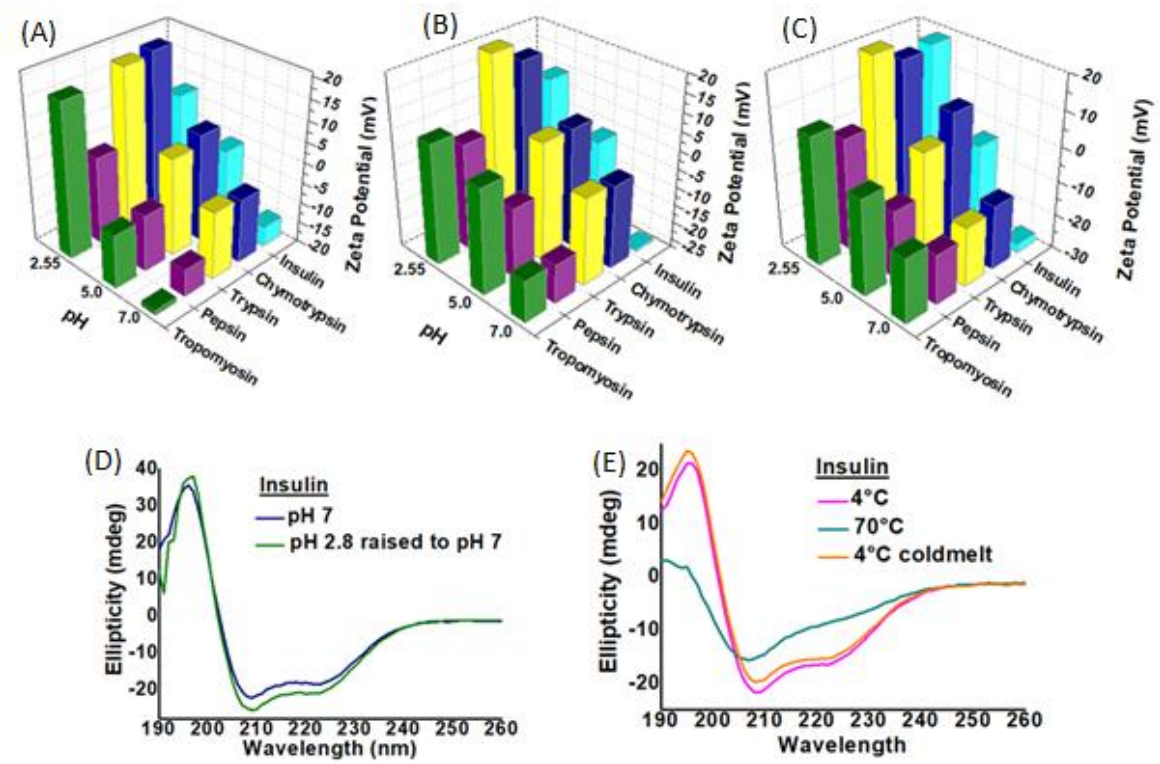

Figure 6.6: Zeta potential and circular dichroism studies of proteins. (A) Zeta Potential of proteins at different pH (2.55,5,7) and 20°C (B) Zeta Potential of proteins at different pH (2.55,5,7) and 37°C (C) Zeta Potential of proteins at different pH (2.55,5,7) and 70°C (D) Circular Dichroism spectra of Insulin at pH 2.8 (pI=5.3) with a slow increment to pH 7 and reverse pH back to 2.8 (E) Circular Dichroism spectra of Insulin at pH 2.8 (below its pI=5.3) for assessing structural changes by subjecting insulin to a temperature reversible cycle

Similar CD data was collected for BSA to see the structural changes when it was bound to GO to form the conjugates. First, the CD spectrum of BSA at pH 3 was recorded for reference. Slowly the protein incubation temperature was increased to 90°C above the protein pI (Figure 6.7A). From the Figure, it is observed that most of the native protein structure gets retained. Similarly, BSA that formed conjugates with GO was assessed for the retention of its primary conformation (Figure 6.7B). Spectra of BSA (pH 3) incubated with GO were recorded at room temperature (25°C), slowly raised to 70°C above its pI and then the mixture slowly cooled back to 25°C. There is

not a significant change from the first set of spectra. The minute changes may be accounted by the functional groups involved in the formation of conjugates with GO. The innate protein conformation is definitely altered slightly by the change in bond lengths guided by the electrostatic potential across the structure that must get resolved to solve entropy and minimize the free energy. This change is not very significant as such changes are common even for the same protein kept at different pH (Figure 6.7C). The protonated form extends in solution differently to the deprotonated form depending on the charge and energy distribution of the molecule. This level of conformity change is similar for BSA and GO conjugates when the pH is reversed to 7 and the temperature of the conjugate is increased to 70°C (Figure 6.7D). From this data, it can be inferred that even after participating in the protein-GO conjugate formation, the protein remains undisturbed to exploit its functional role for various applications. Only GO in different pH buffer/temperature conditions was also studied for reference and was found to give no contribution to the protein signal evident by the straight line (Figure 6.7E).

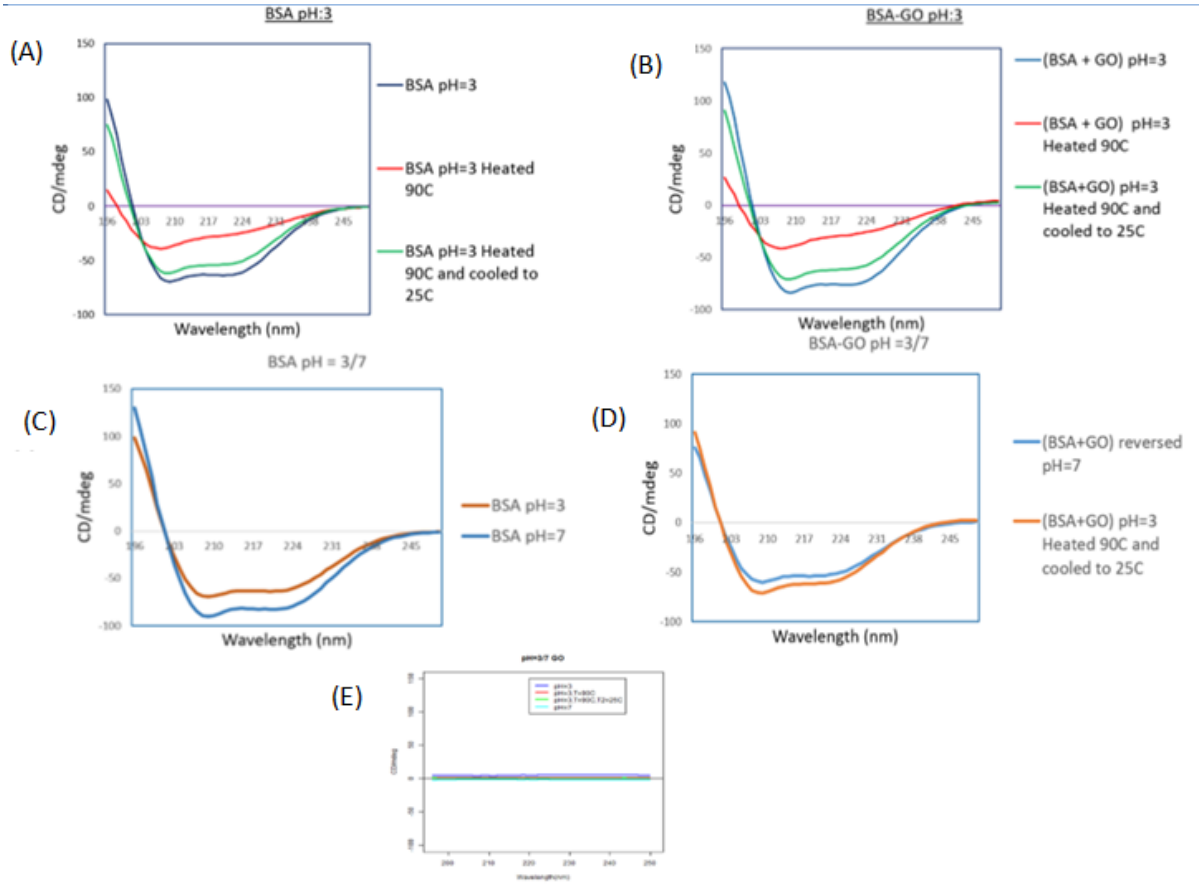

Figure 6.7: Circular Dichroism Spectra Studies for Understanding BSA-GO conjugate formation (A) CD spectra of BSA only at pH 3 subjected to a temperature cycle (25°C-70°C-25°C) (B) CD spectra of BSA-GO at pH 3 subjected to a temperature cycle (25°C-70°C-25°C) (C) CD spectra of BSA in buffers of pH3 and pH 7 (D) BSA-GO subjected to pH(3-7) and temperature (25°C-70°C-25°C) cycle (E) CD spectra of GO only at different temperature and pH

6.2.4 Design of pH-reversible Protein-GO Conjugates for Drug Delivery

The possibility of using protein-GO conjugates as effective oral protein drug vessels was explored. It was evident from the data that only protein in any buffer solution and with GO in a suitable buffer presented homogenous distribution of the protein (Figure 6.8A). The difference on forming protein-GO conjugates laid in the fact that the strong electrostatic interactions between the protein and the graphitic sheets helped in shielding the protein molecules from any denaturants in the external environment. To test this hypothesis, an SDS polyacrylamide gel electrophoresis

experiment was carried out using all possibilities in the different lanes. Two sets of gels were run, one with samples incubated at an acidic pH (pH 3) and the other at neutral pH (pH 7). Both sets were tested for similar samples consisting of protein and GO only respectively and then both incubated together with temperature increment for protein unfolding and without. Additionally, pepsin was added to naked protein and protein-GO conjugate mixture to check the degree of protein digestion by the enzyme. It was observed that only in the case of protein incubated in acidic buffer by slowly heating it above its melting temperature it effectively formed conjugates with GO and got shielded from digestion attack of pepsin enzyme (Figure 6.8B).

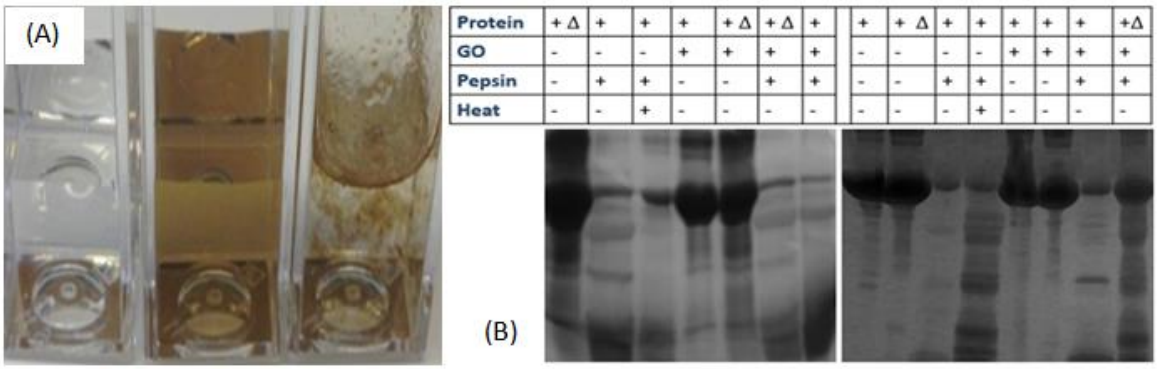

Figure 6.8: Proteolytic Resistance of Protein-GO Conjugates. (A) Protein (BSA) in soluble form in buffer and GO solution, formation of protein-GO conjugates visible on reducing pH below pI (pH 4.7) and heating above the melting temperature of the protein (B) SDS Gel electrophoresis above and below protein pI (pH 3 and pH 7) to check the proteolytic resistance of the protein-GO conjugates using pepsin

This proves how robust and simple such drug delivery systems are for oral delivery of a protein which otherwise is hydrolysed by the stomach and intestinal digestive enzymes. The plasma pH (pH 7.4) supports the re-dissociation of the protein-GO conjugates for the delivery of the protein. Such facile formulations open up the possibility of using a myriad of proteins for oral drug delivery that are otherwise only incorporated through the intravenous route. No complicated additional complementary

ligands are required for such design. GO is biocompatible at low concentrations as its organic composition is very similar to natural biomolecules and to the composition of the body.

6.3 Conclusions

As a novel 2D carbon material with functional groups, GO is an ideal substrate for protein immobilization. In summary, the molecular interaction between a very important biomolecule, protein, was investigated thoroughly with GO. On the basis of different qualitative and quantitative data, various facets of these interactions have been illuminated. It has been demonstrated that electrostatic interactions between an amino acid/peptide/protein having an overall positive charge and GO drive the formation of visible conjugates in solution. This phenomenon has been used for designing pH-reversible protein-GO conjugates for drug delivery. These conjugates provide a promising platform for drug delivery applications through the oral route without proteolytic degradation by the effective shielding effect of GO on the proteins. This work provides important insights, nonetheless further experiments are needed to be done to elucidate this mechanism further and test this hypothesis *in vitro* and *in vivo*. This understanding is crucial as applications for delivery of proteins like insulin through the oral route will revolutionise the current market.

6.4 References

[1] K. S. Novoselov, A. K. Geim, S. V. Morozov, D. Jiang, Y. Zhang, S. V. Dubonos, I. V. Grigorieva, A. A. Firsov. Electric Field Effect in Atomically Thin Carbon Films, Science, 306 (2004) pp. 666–669. Doi:10.1126/science.1102896

[2] W. Hu, C. Peng, M. Lv, X. Li, Y. Zhang, N. Chen, C. Fan, Q. Huang. Protein Corona-Mediated Mitigation of Cytotoxicity of Graphene Oxide, ACS Nano, 5 (2011) pp. 3693–3700

[3] C. Li, J. Adamcik, & R. Mezzenga. Biodegradable nanocomposites of amyloid fibrils and graphene with shape-memory and enzyme-sensing properties. Nature Nanotechnology, 7(2012) 421–427. Doi:10.1038/nnano.2012.62

[4] M. Yan, Q. Liang, W. Wan, Q. Han, S. Tan and M. Ding. Amino acid-modified graphene oxide magnetic nanocomposite for the magnetic separation of proteins. RSC Adv., 7 (2017) 30109

[5] J. Li, S. Wang, D. Zhang, X. Ni and Q. Zhang. Amino Acids Functionalized Graphene Oxide for Enhanced Hydrophilicity and Antifouling Property of Poly(vinylidene fluoride) Membranes. Chinese J.of Pol Sci, 34 (2016) 805-819

[6] Y. Zhang, C. Wu , S. Guo and J. Zhang. Interactions of graphene and graphene oxide with proteins and peptides, Nanotechnol Rev; 2 (2013) pp. 27–45

[7] B. J. Min, C. Lee and H. K. Jeong. Plane Wave Density Functional Theory Studies of the Structural and the Electronic Properties of Amino Acids Attached to Graphene Oxide via Peptide Bonding, J. Korean Phys. Soc., 67 (2015) 507–511. Doi:10.3938/jkps.67.507

[8] M. Simsikova and T. Sikola, Interaction of Graphene Oxide with Proteins and Applications of their Conjugates, J. Of Nanomed. Res., 5 (2017) 109

[9] J. Kuchlyan, N. Kundu, D. Banik, A. Roy and N. Sarkar. Spectroscopy and Fluorescence Lifetime Imaging Microscopy To Probe the Interaction of Bovine Serum Albumin with Graphene Oxide, Langmuir, 31 (2015) 13793−13801

[10] M. Feng, H. Kang, Z. Yang, B. Luan and R. Zhou. Potential Disruption of protein-protein interactions by graphene oxide, J. Chemical Physics 144 (2016) 225102

[11] S. Li, J. J. Mulloor, L. Wang, Y. Ji, C. J. Mulloor, M. Micic, J. Orbulescu and R. M. Leblanc. Strong and Selective Adsorption of Lysozyme on Graphene Oxide, ACS Appl. Mater. Interfaces, 6 (2014) 5704−5712

[12] Li, Shanghao, Analysis of the Interactions between Graphene Oxide and Biomolecules and Protein Fibrillation Using Surface Chemistry and Spectroscopy, Open Access Dissertations (2014) 1253

[13] K. Dave and M. Dhayal. Fluorometric estimation of amino acids interaction with colloidal suspension of FITC functionalized graphene oxide nanoparticles, Appl. Surface Sc. 396 (2017) 978–985

[14] S. Pandit and M. De. Interaction of Amino Acids and Graphene Oxide: Trends in Thermodynamic Properties, J. Phys. Chem. C 121 (2017) 600−608

[15] K. P. Singh, L. Baweja, O. Wolkenhauer, Q. Rahman, S. K. Gupta. Impact of graphene-based nanomaterials (GBNMs) on the structural and functional conformations of hepcidin peptide, Journal of Computer-Aided Molecular Design 32 (2018) 487–496

[16] J. Liu, S. Fu, B. Yuan, Y. Li and Z. Deng. Toward a Universal "Adhesive Nanosheet" for the Assembly of Multiple Nanoparticles Based on a Protein-Induced Reduction/Decoration of Graphene Oxide, J. Am. Chem. Soc. 132 (2010) 7279–7281

[17] X. Wei, L. Hao, X. Shao, Quan Zhang, X. Jia, Z. Zhang, Y. Lin and Q. Peng. Insight into the Interaction of Graphene Oxide with Serum Proteins and the Impact of the Degree of Reduction and Concentration ACS Appl. Mater. Interfaces 7 (2015) 13367−13374

[18] Kenry, K. P. Loha and C. T. Lim. Molecular interactions of graphene oxide with human blood plasma proteins, Nanoscale, 8 (2016) 9425

[19] T. Huang, N. Chiu and H. Lai. Kinetic Analysis of Graphene Oxide Sheet and Protein Interactions Using Surface Plasmon Resonance Biosensors, Conference on Lasers and Electro-Optics Pacific Rim (CLEOPR). (2013) doi:10.1109/cleopr.2013.6600344

[20] S. Li, A. N. Aphale, I. G. Macwan, P. K. Patra, W. G. Gonzalez, J. Miksovska and R. M. Leblanc. Graphene Oxide as a Quencher for Fluorescent Assay of Amino Acids, Peptides, and Proteins, ACS Appl. Mater. Interfaces 4 (2012) 7069−7075

[21] K. Das, K. Rawat, R. Patel and H. B. Bohidar, Size-dependent CdSe quantum dot–lysozyme interaction and effect on enzymatic activity, RSC Adv., 6 (2016) 46744

[22] S. Mondal, R. Thirupathi, L. P. Raoac and H. S. Atreya. Unraveling the dynamic nature of protein–graphene oxide interactions, : RSC Adv., 6 (2016) 52539

[23] H. Li, K. Fierens, Z. Zhang, N. Vanparijs, M. J. Schuijs, K. V. Steendam, N. F. Gracia, R. D. Rycke, T. D. Beer, A. D. Beuckelaer, S. D. Koker, D. Deforce, L. Albertazzi, J. Grooten, B. N. Lambrecht and B. G. D. Geest Spontaneous Protein Adsorption on Graphene Oxide Nanosheets Allowing Efficient Intracellular Vaccine Protein Delivery, ACS Appl. Mater. Interfaces 8 (2016) 1147−1155

[24] H. T. Larijani, M. D. Ganji and M. Jahanshahi. Trends of amino acid adsorption onto graphene and graphene oxide surfaces: a dispersion corrected DFT study, RSC Adv., 5 (2015) 92843